[CANCER RESEARCH 63, 8188–8196, December 1, 2003]

Short Telomeres and Ataxia-Telangiectasia Mutated Deficiency Cooperatively Increase Telomere Dysfunction and Suppress Tumorigenesis

Ling Qi,[1] Margaret A. Strong,[1] Baktiar O. Karim,[2] Mary Armanios,[3] David L. Huso,[2] and Carol W. Greider[1,3]

[1]Departments of Molecular Biology and Genetics, [2]Comparative Medicine, and [3]Oncology, The Johns Hopkins University School of Medicine, Baltimore, Maryland

ABSTRACT

To examine the role of ataxia-telangiectasia mutated (Atm) in telomere function, we generated Atm and telomerase null mice ($Atm^{-/-}$ $mTR^{-/-}$ iG6 mice). These mice exhibited increased germ cell death and chromosome fusions compared with either $Atm^{-/-}$ or $mTR^{-/-}$ iG6 mice. Furthermore, the $Atm^{-/-}$ mTR^{--} iG6 mice had a delayed onset and reduced incidence of thymic lymphoma compared with $Atm^{-/-}$ mice. The tumors in the $Atm^{-/-}$ $mTR^{-/-}$ iG6 mice showed increased apoptosis and anaphase bridges. Finally, lymphomas from $Atm^{-/-}$ $mTR^{-/-}$ iG6 mice were derived from CD8 immature, single-positive T cells, whereas $Atm^{-/-}$ lymphomas were from $CD4^+CD8^+$ double-positive T cells. We propose that Atm protects short telomeres and that Atm deficiency cooperates with short telomeres, leading to increased cell death, decreased tumorigenesis, and increased overall survival.

INTRODUCTION

Chromosomal rearrangement and instability can initiate tumor formation. Cancer cells accumulate genetic changes because of loss of checkpoint controls that normally ensure genomic integrity. Telomeres protect chromosome ends from rearrangement, and loss of telomere function may play an important role in fueling genomic instability in cancer (1–5). In addition to promoting carcinogenesis, telomere dysfunction can also limit tumor growth (4, 6, 7). Dysfunctional telomeres activate cellular DNA damage responses and induce cell cycle arrest, apoptosis, or senescence (3, 8, 9). The telomerase null mouse, $mTR^{-/-}$, shows progressive telomere shortening from the first null generation, $mTR^{-/-}$ G1, through the sixth generation of interbreeding, $mTR^{-/-}$ G6. Although the early generations, $mTR^{-/-}$ G1–G3, show few abnormal phenotypes, the later-generation mice, $mTR^{-/-}$ G4–G6, have critically short telomeres and exhibit germ cell apoptosis and infertility (10, 11), increased genomic instability, and cancer predisposition (1–5). However, the underlying mechanisms of response to dysfunctional telomeres are not yet understood but are under active investigation.

A-T[4] is a pleiotropic genetic disorder attributable to recessive mutations in *ATM* (12, 13). It is characterized by cerebellar degeneration, immunodeficiency, radiosensitivity, and cancer predisposition, particularly lymphoid malignancies (14). The ATM family of protein kinases, which includes ATR and their yeast homologs Tel1 and Mec1/Rad3, plays a critical role in the cellular response to DNA damage (15, 16). In the presence of DNA damage, ATM and ATR phosphorylate downstream targets including NBS, BRCA1, and p53 (15–19). In addition, ATM plays a direct role in telomere maintenance. Loss of the ATM homolog Tel1 in yeast leads to short telomeres (20–24). Similarly, human A-T cells have shorter telomeres than normal cells (25). Finally, ATM may play a role in the cellular response to dysfunctional telomeres. Overexpression of a dominant-negative form of the telomere-binding protein TRF2 induces apoptosis in normal lymphocytes but not in lymphocytes from A-T patients (8).

To study the interplay between Atm and telomeres in telomere function and tumorigenesis, we generated double-knockout mice with short telomeres lacking *Atm* ($Atm^{-/-}$ $mTR^{-/-}$ iG6). Several lines of Atm mutant mice have been described. Although these Atm mutant mouse models recapitulate some features of the A-T patients, the phenotypes of these mouse models vary (26–30), likely because of a different genetic background and/or the different regions of the Atm protein that were targeted. For example, the $Atm^{-/-}$ mice generated by Barlow *et al.* (26) on a 129S6/SvEvTac background develop thymic lymphoma at 12–16 weeks of age. In contrast, the Atm mutant mice $Atm^{y/y}$ generated by Borghesani *et al.* (29) on a 129Sv/C57BL6 background develop thymic lymphoma at much lower frequency with a longer latency and have a median survival time of over 52 weeks. The increased tumor latency in the latter case may be attributable to the expression of a low level of mutant Atm mRNA with an intact kinase domain in the $Atm^{y/y}$ mutant mice (29). Recently, Wong *et al.* (31) crossed $mTR^{-/-}$ mice onto $Atm^{y/y}$ mice and showed increased cell death in bone marrow cell culture and gastrointestinal crypts in the double-mutant mice. The incidence of thymic lymphoma was decreased, but the survival of these mice was not changed.

We used the Atm mutant mouse model generated by Barlow *et al.* (26) and adopted a different crossing scheme than Wong *et al.* (31). Consistent with Wong *et al.* (31), we also found increased cell death and reduced tumorigenesis in the double-mutant mice. Furthermore, we observed the cooperative effect of Atm deficiency and short telomeres on telomere dysfunction without extensive telomere shortening and an increased survival rate of double-mutant mice. We examined possible mechanisms for the increased survival and found that increased apoptosis and altered T-cell development contribute to decreased tumor growth. Finally, our data suggest a role for Atm in protecting short telomeres.

MATERIALS AND METHODS

Mice. $mTR^{+/-}$ mice on a C57BL/6 background were generated as described (10). $Atm^{+/-}$ mice (The Jackson Laboratory) on a 129S6/SvEvTac background (26) were mated to $mTR^{+/-}$ mice to generate double-heterozygous $Atm^{+/-}$ $mTR^{+/-}$ mice. The $Atm^{+/-}$ $mTR^{+/-}$ mice were intercrossed to generate $Atm^{+/+}$ $mTR^{+/+}$ and $Atm^{-/-}$ $mTR^{+/+}$ mice. $Atm^{-/-}$ $mTR^{-/-}$ iG6 mice were generated by intergenerational crosses: $Atm^{+/-}$ $mTR^{+/-}$ mice were crossed with $mTR^{-/-}$ G4 mice to first generate $Atm^{+/-}$ $mTR^{-/-}$ iG5 mice. These mice were then intercrossed to generate $Atm^{-/-}$ $mTR^{-/-}$ iG6 mice. The $Atm^{-/-}$ $mTR^{-/-}$ iG6 and $Atm^{-/-}$ $mTR^{+/+}$ control mice are on the same genetic background. Genotyping was done by PCR as described previously for *Atm* (26) and *mTR* (32). All of the animals were maintained in a pathogen-free facility, weighed every week, and checked every other day for signs of

Received 8/14/03; revised 10/6/03; accepted 10/16/03.

Grant support: NIH Grants RR00171 (to D. L. H.) and CA16519 (to C. W. G.). L. Q. is the second Dr. George Santos Researcher and postdoctoral fellow of the Leukemia and Lymphoma Society (5532-03). B. O. K. is supported by NIH Training Grant RR07002.

The costs of publication of this article were defrayed in part by the payment of page charges. This article must therefore be hereby marked *advertisement* in accordance with 18 U.S.C. Section 1734 solely to indicate this fact.

Notes: Supplementary data for this article are available at Cancer Research Online (http://cancerres.aacrjournals.org). M. A. S. and B. O. K. contributed equally to this work.

Requests for reprints: Carol Greider, 617 Hunterian, 725 North Wolfe Street, Baltimore, MD 21205. Phone: (410) 614-6506; Fax: (410) 614-2987; E-mail: cgreider@jhmi.edu.

[4] The abbreviations used are: A-T, ataxia-telangiecstasia; Atm (ATM), ataxia-telangiectasia mutated; Atr (ATR), ATM- and Rad 3-related; mTR, mouse telomerase RNA; iG, intergenerational; TUNEL, terminal deoxynucleotidyl transferase-mediated nick end labeling; GCNA1, germ cell nuclear antigen 1; PCNA, proliferating cell nuclear antigen; IL, interleukin; Q-FISH, quantitative fluorescence in situ hybridization; SKY, spectral karyotyping; BrdUrd, bromodeoxyuridine; TCR, T cell receptor.

sickness. All mouse protocols were approved by the Institutional Care and Use Committee at the Johns Hopkins University School of Medicine.

Histopathology Examination. When a mouse was sacrificed, its internal organs were fixed in 10% formalin, and the rest of the mouse (skeleton, testis, etc.) was fixed in Bouin's solution. After being embedded in paraffin, 5-μm tissue sections were stained with H&E. The testis sections from 7- to 10-week-old mice were examined and photographed using a Nikon inverted microscope ECLIPSE TE300 with SPOT RT software (Diagnostic Instruments, Inc.). Over 100 tubules for each mouse were counted and classified into four categories (normal, hypospermatogenesis, germinal arrest, and Sertoli cell only) by two independent investigators. For the metastasis analysis, pathological diagnoses were determined by two independent pathologists as a blind study.

Immunofluorescence and TUNEL Assay. Sections were deparaffinized and hydrated as described previously (11). For GCNA1 and PCNA staining, sections were stained after antigen retrieval with 1 mM EDTA with GCNA1 [undiluted; from G. C. Enders, University of Kansas, Kansas City, KS (38)], followed by goat anti-rat IgM Cy3 (1:400; Jackson ImmunoResearch), PCNA C-20 (1:100; Santa Cruz Biotechnology), followed by donkey anti-goat IgG Cy3 (1:300; Jackson ImmunoResearch). TUNEL assay was performed using the TUNEL kit (Roche) per the manufacturer's procedure. Four low-power-field pictures (×200) were taken for each thymic lymphoma sample, and TUNEL-positive cells were counted as a blind study.

Metaphase Preparation. Metaphases from spleen, thymus, and bone marrow were generated as described previously (33). In brief, splenocytes and thymocytes were cultured in the presence of 5 μg/ml ConA + 20 μg/ml lipopolysaccharide, 750 ng/ml ionomycin + 20 ng/ml phorbol myristate acetate + 10 units/ml of IL-2, respectively, for 48 h before being harvested for metaphase preparation. To obtain bone marrow metaphases, mice received injections of 0.1 ml of 0.5% colchicine (Sigma) for 45min before being sacrificed. Bone marrow cells were obtained by flushing femurs and tibias with fresh 75 mM KCl and incubated at 37°C for 15 min, followed by fixation four times in fresh 3:1 methanol:glacial acetic acid.

Q-FISH and SKY. Q-FISH and SKY were performed on the same sets of metaphases as described previously (34, 35). The analysis of chromosome abnormalities (signal-free ends, translocations, fusions, and fragments) was carried out as a blind study. To avoid counting chromosome fragments as signal-free ends, the size of each chromosome lacking a telomere signal was closely compared with its homolog using SKY. If the chromosome was shorter than its homolog, the event was scored as a fragmentation and not as a signal-free end. Each chromosome fusion was identified by SKY, and the identity of all chromosome fusions was counted directly. In addition, to avoid overestimating the clonal events, each specific chromosome fusion in a given mouse was counted as one independent fusion event.

Kaplan-Meier Survival Curve. If the mouse dropped 20–40% of its body weight in a 3-day interval and was motionless with dramatic trembling or other signs of ill health, it was pronounced dead and evaluated by a complete pathological examination.

Mitotic Figures and Anaphase Bridges. The measurement of mitotic figures and the anaphase bridge index in the thymic lymphoma sections was counted as a blind study by two independent investigators. A total of 10 high-power fields (×600) were counted in each sample. Anaphase bridges were defined as one or more lines spanning two separating anaphase poles.

BrdUrd Labeling. Mice at 7–10 weeks with no signs of sickness received injections i.p. of BrdUrd (0.6 mg/10g body weight). One hour later, mice were sacrificed, and bone marrow cells were flushed out from the femurs and tibias using PBS. Cells were then fixed in cold 70% ethanol and stored overnight at −20°C. All of the following steps were done at room temperature. After being treated with 50 units/ml of DNase (Roche) in 4.2 mM $MgCl_2$/150 mM NaCl for 10 min, cells were incubated with anti-BrdUrd-FITC (BD PharMingen; no dilution) for 30 min. Cells were then resuspended in 20 μg/ml of 7-amino-actinomycin D (Molecular Probes) for 30 min before being analyzed using the CELLQUEST program (BD).

Flow Cytometric Analysis. Single-cell suspensions were prepared from thymus or thymic lymphoma. After being washed once in PBS/2% BSA, cells were stained with antibodies for 15 min at room temperature before the analysis using the CELLQUEST program. Antibodies purchased from BD PharMingen were as follows: CD4-FITC (RM4-5, 1:200), CD8-PE (53-6.7, 1:200), CD3-Cychrome (145-2C11, 1:200) or CD8-FITC (53-6.7, 1:200), TCR β-PE (H57-597, 1:200), CD4-Cychrome (RM4-5, 1:300).

RESULTS

Generation of $Atm^{-/-}$ Mice with Short Telomeres Using Intergenerational Cross. Because it is the shortest telomere that triggers the cellular response to dysfunctional telomeres (33), we used an intergenerational breeding method to introduce short telomeres into $Atm^{-/-}$ mice. $Atm^{+/-}$ $mTR^{+/-}$ mice were crossed with fourth generation (G4) $mTR^{-/-}$ mice. The resulting progeny, $Atm^{+/-}$ $mTR^{-/-}$ iG5 (iG5 refers to the progeny of intergenerational crosses) were then intercrossed to obtain $Atm^{+/+}$ $mTR^{-/-}$ iG6 and $Atm^{-/-}$ $mTR^{-/-}$ iG6 mice. The litter size resulting from this cross was only 2.8 ± 1.4 pups/litter, which is significantly less than the 7.3 ± 2.8 pups/litter for the cross that generated $Atm^{+/-}$ $mTR^{-/-}$ iG5 mice (20 litters; $P = 0.0001$), indicating that short dysfunctional telomeres lead to a loss of fertility as shown previously in the late-generation $mTR^{-/-}$ mice (10).

Increased Germ Cell Death in the $Atm^{-/-}$ $mTR^{-/-}$ iG6 Mice. To determine whether Atm is required for sensing telomere dysfunction, we examined germ cell death by assaying seminiferous tubule morphology. Late-generation $mTR^{-/-}$ mice show germ cell apoptosis and seminiferous tubule atrophy (10, 11). In $Atm^{-/-}$ mice, germ cells arrest and accumulate at the leptotene-pachytene stage of meiosis (27, 36). In $Atm^{+/+}$ $mTR^{-/-}$ iG6 mice, 6.5% of the tubules were atrophic and showed a Sertoli cell only phenotype (Ref. 37; Fig. 1, *A* and *C*). Notably, there was a more severe phenotype in $Atm^{-/-}$ $mTR^{-/-}$ iG6 mice with 78% of the tubules lacking germ cells (Fig. 1, *A* and *C*). The tubules that were not empty (~22%) showed the germinal arrest characteristic of $Atm^{-/-}$ $mTR^{+/+}$ mice (Fig. 1, *A* and *C*).

To further measure the extent of germ cell loss, we stained testis sections for GCNA1, which is abundantly expressed in spermatogonia and primary spermatocytes (38). There was a significant reduction in GCNA1 staining in the $Atm^{-/-}$ $mTR^{-/-}$ iG6 mice compared with wild-type mice and both single null mutant mice (Fig. 1, *B* and *C*). In addition, staining for PCNA, a marker of mitotic and premeiotic precursors (39), also showed extensive cell loss in $Atm^{-/-}$ $mTR^{-/-}$ iG6 (Fig. 1*C*). This tubule atrophy is not likely attributable to growth defects of the $Atm^{-/-}$ $mTR^{-/-}$ iG6 mice because at 7–10 weeks, these mice were of the same average size and grew at a rate similar to $Atm^{+/+}$ $mTR^{-/-}$ iG6 mice (see Fig. 4*B* below). Therefore, unlike in $p53^{-/-}$ $mTR^{-/-}$ late-generation mice (3), tubule atrophy was not rescued by loss of Atm. We conclude that Atm is not essential for germ cell death in response to short telomeres. A similar conclusion was reached recently by Wong *et al.* (31) from their analysis of apoptosis in bone marrow cell culture and intestinal crypts in $Atm^{y/y}$ $mTR^{-/-}$ mice. Furthermore, the significant increase in seminiferous tubule atrophy in $Atm^{-/-}$ $mTR^{-/-}$ iG6 mice compared with either $Atm^{-/-}$ $mTR^{+/+}$ or $Atm^{+/+}$ $mTR^{-/-}$ iG6 suggests that Atm deficiency, together with short telomeres, accentuates telomere dysfunction.

Telomere-length Independent Cooperative Effect of Atm Deficiency and Short Telomeres. To determine whether the increased telomere dysfunction was telomere length dependent, we performed Q-FISH on metaphase chromosome spreads from lymphocytes of 7–10 week old mice to measure the change in telomere length. There was a slight reduction in average telomere length in $Atm^{-/-}$ $mTR^{+/+}$ compared with wild-type mice (Fig. 2*B*), consistent with the shortening seen in human A-T cells (25). Similarly, $Atm^{-/-}$ $mTR^{-/-}$ iG6 mice showed only a slight decrease in telomere length compared with $Atm^{+/+}$ $mTR^{-/-}$ iG6 mice (Fig. 2*D*). Because the shortest telomere triggers apoptosis (33), we quantitated the number of signal-free chromosome ends in $Atm^{-/-}$ $mTR^{-/-}$ iG6 and $Atm^{+/+}$ $mTR^{-/-}$ iG6 mice. To distinguish chromosome fragments from signal-free ends, we used FISH along with SKY. When fragments were eliminated, we

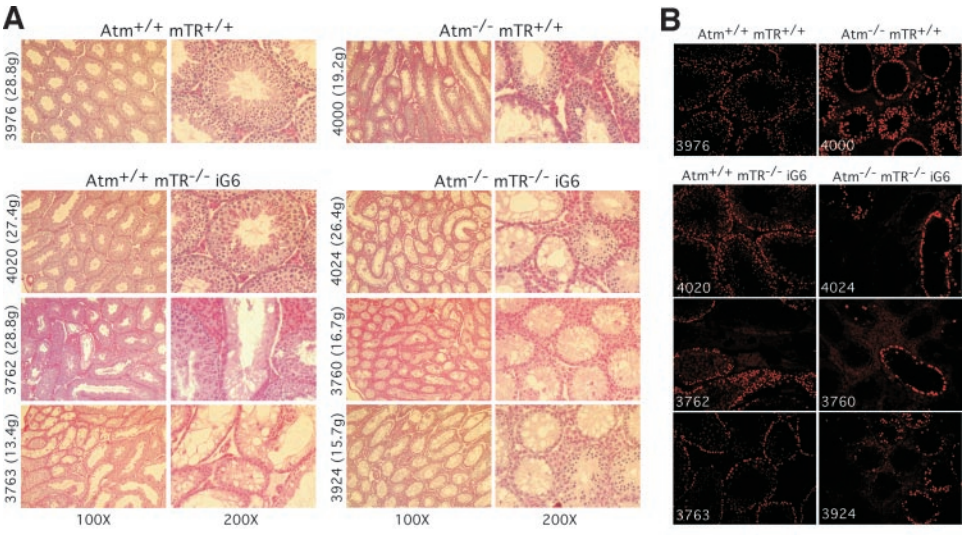

Fig. 1. Short telomeres lead to germ cell depletion in the absence of ATM. *A*, H&E-stained testis sections (7–10 week-old) are shown for the genotypes indicated at the *top* of each panel. The mouse numbers are indicated at the *left*, and the body weight of the mouse is indicated in *parentheses*. Pictures were taken at ×100 and ×200. *B*, immunofluorescent staining of GCNA1 in testis sections labeled as in *A*. One representative sample is shown for $Atm^{+/+}$ $mTR^{+/+}$ and $Atm^{-/-}$ $mTR^{+/+}$ mice. Three representative samples are shown for $Atm^{+/+}$ $mTR^{-/-}$ iG6 and $Atm^{-/-}$ $mTR^{-/-}$ iG6 mice. *C*, summary of testis morphology for each genotype. Seminiferous tubules (100–200) from each mouse were classified into four categories based on H&E staining: normal, hypospermatogenesis, germinal arrest, and Sertoli cell only. The percentages of $PCNA^+$ and $GCNA1^+$ tubules in immunofluorescent images were counted. The average number is shown. *n*, the number of mice for each genotype.

C

Mouse genotype (n=number of mice)	Percentage of total tubules (out of 100-200 tubules)					
	Normal[a]	Hypo-spermatogenesis[b]	Germinal Arrest[c]	Sertoli cell only[d]	$PCNA^+$	$GCNA1^+$
$Atm^{+/+}$ $mTR^{+/+}$ (n=4)	100*	0	0	0	100*	100*
$Atm^{-/-}$ $mTR^{+/+}$ (n=7)	0	0	98.5±1.4*	1.5±1.4*	91.4±4.5*	95.6±2.8*
$Atm^{+/+}$ $mTR^{-/-}$ iG6 (n=6)	90.1±9.4*	3.5±3.5	0	6.5±7.6*	91.3±5.0*	90.5±7.2*
$Atm^{-/-}$ $mTR^{-/-}$ iG6 (n=5)	0	0	21.5±25.1	78.3±25.1	15.5±12.3	21.8±18.7

* indicates significant difference compared to $Atm^{-/-}$ $mTR^{-/-}$ iG6 mice (*P*-values by Student's t-test are < 0.01).
[a]Tubules have all stages of spermatogenesis. [b]Tubules are hypocellular and contain some but not all stages of spermatogenesis. [c]Tubules have arrested spermatocytes and no spermatozoa. [d]Tubules show only Sertoli cells.

found no significant difference in signal-free ends in $Atm^{-/-}$ $mTR^{-/-}$ iG6 lymphocytes compared with $Atm^{+/+}$ $mTR^{-/-}$ iG6 ($P = 0.46$). Although overall telomere length was not measured by Wong *et al.* (31), they did report an increase in signal-free ends. The different results may be attributable to the methods used to exclude chromosome fragments from the analysis or different Atm mutant mouse models. Our study suggests that telomere shortening is not likely to account for the increased telomere dysfunction in the $Atm^{-/-}$ $mTR^{-/-}$ iG6 mice.

Chromosome Instability Induced by Increased Telomere Dysfunction. Next, we examined the impact of Atm deficiency and short telomeres on chromosomal rearrangements using SKY. A high rate of chromosome fusions was seen in both $Atm^{-/-}$ $mTR^{-/-}$ iG6 and $Atm^{+/+}$ $mTR^{-/-}$ iG6 animals (Table 1). In contrast, only one fusion was present in the *Atm* single null mice (Table 1), suggesting that loss of Atm alone does not lead to telomere dysfunction. Although the total number of fusion events was higher in the $Atm^{+/+}$ $mTR^{-/-}$ iG6 mice compared with the $Atm^{-/-}$ $mTR^{-/-}$ iG6 littermates (Table 1), this increase was primarily attributable to the clonal expansion of two fusion events, 12p;14p and 9p;14p (Fig. 3*C*). Although they are likely clonal, these two fusions do not represent germ-line events because they were not present in all metaphases from one given mouse (data not shown). To avoid overrepresenting clonal fusion events, we quantitated the number of fusions between specific chromosomes in each mouse as "independent fusion events" (Table 1 and Fig. 3*C*). The spectrum of chromosomes involved in independent fusion events differed significantly between $Atm^{+/+}$ $mTR^{-/-}$ iG6 and $Atm^{-/-}$ $mTR^{-/-}$ iG6 mice (Fig. 3*C*). Although all fusions in $Atm^{+/+}$ $mTR^{-/-}$ iG6 mice were p-arm-to-p-arm, the $Atm^{-/-}$ $mTR^{-/-}$ iG6 mice showed both p-arm-to-p-arm and q-arm-to-q-arm fusions (Fig. 3 and Table 1). In addition, many more independent chromosome ends were involved in fusions in $Atm^{-/-}$ $mTR^{-/-}$ iG6 mice than in $Atm^{+/+}$ $mTR^{-/-}$ iG6 mice (Fig. 3*C*). Of 162 metaphases examined for both genotypes, 25 different chromosome ends were involved in 25 independent fusion events in $Atm^{-/-}$ $mTR^{-/-}$ iG6 mice, whereas only 8 chromosome ends were involved in 12 independent events in $Atm^{+/+}$ $mTR^{-/-}$ iG6 mice (Fig. 3*C*). Finally, there was an expected increase in chromosome fragments and translocations in both $Atm^{-/-}$ $mTR^{+/+}$ and $Atm^{-/-}$ $mTR^{-/-}$ iG6 mice compared with the $Atm^{+/+}$ mice (Table 1), as has been documented previously in $Atm^{-/-}$ mice (26, 40). Therefore, the increase in q;q fusions and the increased number and change in the repertoire of the chromosomes involved in fusion in $Atm^{-/-}$ $mTR^{-/-}$ iG6 mice suggest that loss of Atm function increases telomere dysfunction of short telomeres.

Delayed and Reduced Incidence of Thymic Lymphoma in $Atm^{-/-}$ $mTR^{-/-}$ iG6 Mice. We next determined how dysfunctional telomeres affect tumorigenesis in the Atm background. The majority of $Atm^{-/-}$ mice from this mouse model typically develop thymic lymphoma and die around 16 weeks of age (26–28, 41). In our colony, the median survival time was 15 weeks for $Atm^{-/-}$ $mTR^{+/+}$ mice ($n = 28$; Fig. 4*A*). Strikingly, the $Atm^{-/-}$ $mTR^{-/-}$ iG6 mice had a median survival time of 36 weeks ($P = 0.0009$; Fig. 4A). In total, 47% of the $Atm^{-/-}$ $mTR^{-/-}$ iG6 mice (7 of 15) survived for over 44 weeks (Fig. 4*A*). Thymic lymphomas were found in 7 of 8 $Atm^{-/-}$ $mTR^{-/-}$ iG6 mice that died. A lymphoma of B-cell lineage was observed in one $Atm^{-/-}$ $mTR^{-/-}$ iG6 mouse with an atrophic thymus (Fig. 4*A*, *asterisk*). Thymic lymphoma did not occur in one $Atm^{+/+}$ $mTR^{+/+}$ or $Atm^{+/+}$ $mTR^{-/-}$ iG6 mouse that died (Fig. 4*A*). Histopathological examination revealed lymphoma cells invading a variety of organs including liver, kidney, bone marrow, and skeletal

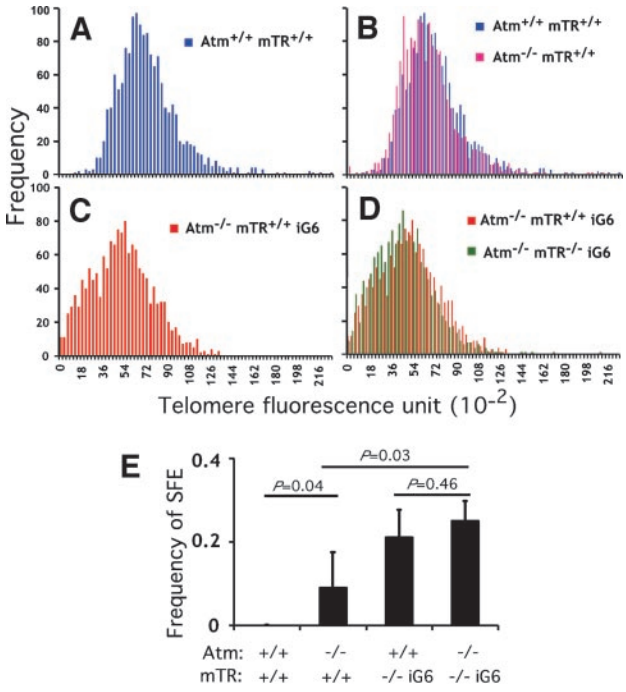

Fig. 2. ATM deficiency has no significant effect on telomere length. *A*, Q-FISH data from $Atm^{+/+}$ $mTR^{+/+}$ are shown in *blue*. *B*, the data from *A* are shown overlayed with telomere signals from $Atm^{-/-}$ $mTR^{+/+}$ metaphases shown in *magenta*. The mice examined are littermates from a cross of double heterozygotes. *C*, Q-FISH data from $Atm^{+/+}$ $mTR^{-/-}$ iG6 mice are shown in *red*. *D*, the Q-FISH signal from $Atm^{-/-}$ $mTR^{-/-}$ iG6 (*green*) is overlayed with the data from the $Atm^{+/+}$ $mTR^{-/-}$ iG6 littermates in *red* as in *C*. Overlays are shown to highlight the small difference in telomere length seen in the $Atm^{-/-}$ mice. A total of 18 metaphases (~3,000 telomere signals) were analyzed for each genotype. The data represent three independent experiments with three mice for each genotype. *E*, signal-free ends (*SFE*) were counted manually after overexposing the telomere signal. A total of 75 metaphases from 4 independent $Atm^{+/+}$ $mTR^{+/+}$ mice, 88 metaphases from 5 independent $Atm^{-/-}$ $mTR^{+/+}$ mice, 73 metaphases from 5 independent $Atm^{+/+}$ $mTR^{-/-}$ iG6 mice, and 100 metaphases from 6 independent $Atm^{-/-}$ $mTR^{-/-}$ iG6 mice were analyzed. *Frequency of SFE*, the number of SFE per metaphase per mouse. *Bars*, SD of the means from each mouse of that genotype.

muscle in both $Atm^{-/-}$ $mTR^{+/+}$ and $Atm^{-/-}$ $mTR^{-/-}$ iG6 mice (Supplementary Table 1). In addition to the lymphoid (T- and B-cell) tumors, we also saw ovarian tubulostromal adenoma and squamous cell carcinoma in the dying $Atm^{-/-}$ $mTR^{-/-}$ iG6 mice (Supplementary Table 1). The development of the non-T-cell tumors may be attributable to the increased life span of these mice. A recent study also found a decrease in thymic lymphoma in $Atm^{y/y}$ $mTR^{-/-}$ mice (31), but because the mouse model they used developed thymic lymphoma at a very advanced age (52 weeks; Ref. 29), no increase in life span was seen in that study (see "Discussion").

The increase in survival of the mice was not attributable to the change in growth rate because the growth rates of $Atm^{-/-}$ $mTR^{+/+}$ and $Atm^{-/-}$ $mTR^{-/-}$ iG6 mice were similar (Fig. 4*B*). To further exclude the possibility that extended survival was attributable to the proliferation defects in $Atm^{-/-}$ $mTR^{-/-}$ iG6 cells, we analyzed BrdUrd incorporation in bone marrow cells from healthy, tumor-free mice 7 to 10 weeks of age. No significant difference was found between $Atm^{-/-}$ $mTR^{+/+}$ and $Atm^{-/-}$ $mTR^{-/-}$ iG6 mice (Fig. 4*C*). Similar results were obtained for BrdUrd incorporation in thymocytes and splenocytes from the same mice (data not shown). Thus, the delayed incidence of thymic lymphoma in the $Atm^{-/-}$ $mTR^{-/-}$ iG6 mice was not attributable to general growth or proliferation defects.

Increased Apoptosis in Thymic Lymphoma of $Atm^{-/-}$ $mTR^{-/-}$ iG6 Mice. The delayed incidence of thymic lymphoma in the $Atm^{-/-}$ $mTR^{-/-}$ iG6 mice may result from the cooperative effect of short telomeres and Atm deficiency on apoptosis as we found in the testis. To examine apoptosis directly on thymic lymphoma sections, we used the TUNEL assay. Tumors from $Atm^{-/-}$ $mTR^{-/-}$ iG6 mice ($n = 4$) exhibited significantly more TUNEL-positive cells than those from $Atm^{-/-}$ $mTR^{+/+}$ mice ($n = 6$; $P = 0.01$; Fig. 5*A*). Moreover, unlike $Atm^{-/-}$ $mTR^{+/+}$ thymic lymphomas that were easily cultured *in vitro*, we were not able to establish cultures from $Atm^{-/-}$ $mTR^{-/-}$ iG6 tumors, even in the presence of IL-2 and other mitogens (data not shown). Thus, increased apoptosis, presumably induced by telomere dysfunction, may in part explain the decreased incidence and/or increased latency of thymic lymphoma.

Telomere dysfunction often results in the appearance of anaphase bridges through the formation of dicentric chromosomes (4, 42, 43). To examine telomere dysfunction in tumors, we measured the anaphase bridge index in H&E stained sections of thymic lymphomas from $Atm^{-/-}$ $mTR^{+/+}$ and $Atm^{-/-}$ $mTR^{-/-}$ iG6 mice ($n = 4$ for each genotype). There was a significant increase in the number of anaphase bridges in the $Atm^{-/-}$ $mTR^{-/-}$ iG6 tumor sections (Fig. 5*C*). Over 90% of the anaphases from $Atm^{-/-}$ $mTR^{-/-}$ iG6 mice had at least one bridge in contrast to 37% in the $Atm^{-/-}$ $mTR^{+/+}$ mice ($P = 0.00001$; Fig. 5, *B* and *C*). Thus, the increase in the number of anaphase bridges in the $Atm^{-/-}$ $mTR^{-/-}$ iG6 tumors is consistent with the increased telomere dysfunction.

To determine whether a decrease in tumor cell proliferation also contributed to increased tumor latency, we measured the mitotic index in H&E sections of thymic lymphomas. No significant difference in the number of mitotic figures was seen between $Atm^{-/-}$ $mTR^{+/+}$ and $Atm^{-/-}$ $mTR^{-/-}$ iG6 mice ($n = 4$ for each; $P = 0.23$; Fig. 5*D*). Thus, although we saw no evidence of decreased proliferation of $Atm^{-/-}$ $mTR^{-/-}$ iG6 tumor cells, we did find evidence for increased telomere dysfunction in these tumors.

Transformation of a Different T-Cell Type in $Atm^{-/-}$ $mTR^{-/-}$ iG6 Mice. Thymic lymphomas in $Atm^{-/-}$ mice are positive for both CD4 and CD8 immune T-cell lineage markers (26, 27). The double-positive state of these tumors suggests that they arise early in T-cell development before the transition to more mature, $CD4^+$ or $CD8^+$ single-positive cells. Tumors that arise in double-knockout mice $Atm^{-/-}$ $p21^{-/-}$ and $Atm^{-/-}$ $p53^{-/-}$ (44) and the $NBS1^{m/m}$ mouse (45) also are $CD4^+CD8^+$ double positive. Consistent with early observations, we found that the thymic lymphomas in $Atm^{-/-}$ $mTR^{+/+}$ mice ($n = 5$) were $CD4^+CD8^+$ with either high or low levels of T-cell maturation markers CD3 (Fig. 6*A*) and TCR-β chain (data not shown; Ref. 46). Surprisingly, thymic lymphomas derived from the $Atm^{-/-}$ $mTR^{-/-}$ iG6 mice ($n = 4$) were $CD8^+CD4^-$ and did not express TCR-β/CD3 complex on their surface (Fig. 6*A* and data not

Table 1 *Summary of chromosome abnormalities*

Mouse genotype (n = number of mice)	No. of metaphases	Independent fusion events[a]		Fragments	Translocations
		p;p	q;q		
$Atm^{+/+}$ $mTR^{+/+}$ ($n = 4$)	112	0	0	3	0
$Atm^{-/-}$ $mTR^{+/+}$ ($n = 5$)	101	0	1 (1)	44	15
$Atm^{+/+}$ $mTR^{-/-}$ iG6 ($n = 5$)	162	12 (100)	0	7	0
$Atm^{-/-}$ $mTR^{-/-}$ iG6 ($n = 6$)	162	17 (35)	8 (14)	36	6

[a] One independent fusion event is one specific fusion event in a given mouse. Numbers in parentheses indicate total fusion events scored. p;p indicates p-arm-to-p-arm Robertsonian-type fusion. q;q indicates q-arm-to-q-arm dicentric fusion.

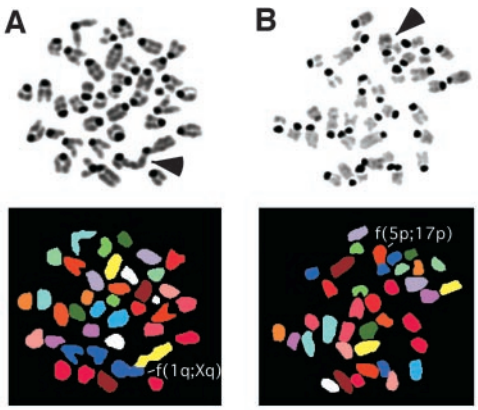

C

Mouse genotype (n=number of mice)	Shared events		Non-shared events	
	Fusion	Numbers	Fusion	Numbers
$Atm^{+/+}$ $mTR^{-/-}$ iG6 (n=5)	9p;9p	1 (3)	2p;15p	1 (1)
	9p;12p	1 (3)	9p;14p	1 (26)
	12p;12p	3 (6)	10p;10p	1 (1)
			12p;14p	3 (58)
			14p;14p	1 (1)
			16p;18p	1 (1)
$Atm^{-/-}$ $mTR^{-/-}$ iG6 (n=6)	9p;9p	1 (1)	1p;17p	1 (1)
	9p;12p	1 (1)	2p;Xp	1 (1)
	12p;12p	2 (6)	3p;14p	1 (1)
			4p;12p	1 (1)
			5p;7p	1 (1)
			5p;17p	1 (3)
			6p;Xp	1 (1)
			11p;Xp	1 (1)
			12p;18p	1 (1)
			12p;Xp	1 (6)
			13p;16p	1 (1)
			18p;Xp	1 (1)
			Xp;Xp	1 (7)
			1q;Xq	1 (1)
			2q;9q	1 (7)
			4q;9q	1 (1)
			4q;12q	1 (1)
			9q;9q	1 (1)
			9q;12q	1 (1)
			14q;18q	1 (2)
			15q;15q	1 (1)

Fig. 3. Increased independent fusion events in the $Atm^{-/-}$ $mTR^{-/-}$ iG6 mice. *A* and *B*, two representative unique fusion events in the $Atm^{-/-}$ $mTR^{-/-}$ iG6 mice indicated by *arrowheads*: *A*, single q-arm fusion f(1q;Xq); *B*, p-arm-to-p-arm fusion f(5p;17p). *C*, summary of independent fusion events. Number indicates independent fusion events scored. Number in the *parentheses* indicates total events scored for the independent fusion event from each genotype. *n* is the number of mice for each genotype.

shown). Despite the lack of surface TCR-β/CD3 expression, PCR analysis using the primers specific for Vβ5.1/Jβ2.6 and Vβ8.2/Jβ2.6 revealed that these cells had undergone V(D)J rearrangement (Supplementary Fig. 1). Thus, these $CD4^-CD8^+$ cells had apparently progressed beyond the $CD4^-CD8^-$ double-negative stage. These cells, however, are not derived from mature $CD8^+$ T cells but rather may represent immature single-positive cells, a stage between the double-negative and the double-positive stages (47–49). When cultured *in vitro*, cells from the $Atm^{-/-}$ $mTR^{-/-}$ iG6 tumors did not respond to a variety of mitogenic stimuli, including phorbol myristate acetate, ionomycin, and IL-2 (data not shown), consistent with their being intermediate, immature, single-positive cells (47, 48, 50). Furthermore, after 24 h of *in vitro* culture, tumor cells differentiated into $CD8^+CD4^{low/+}$ T cells with increased expression of CD3 (Fig. 6*B*), suggesting that these $CD8^+$ cells from $Atm^{-/-}$ $mTR^{-/-}$ iG6 mice are at an earlier developmental stage than the double-positive cells (47, 48, 51, 52).

To exclude the possibility that in the $Atm^{-/-}$ $mTR^{-/-}$ iG6 mice T-cell development was blocked at the $CD8^+$ immature, single-positive stage, we examined T-cell types in thymuses of healthy mice that were 7–10 weeks of age. The percentages of double-positive, double-negative, and single-positive ($CD4^+$ or $CD8^+$) thymocytes

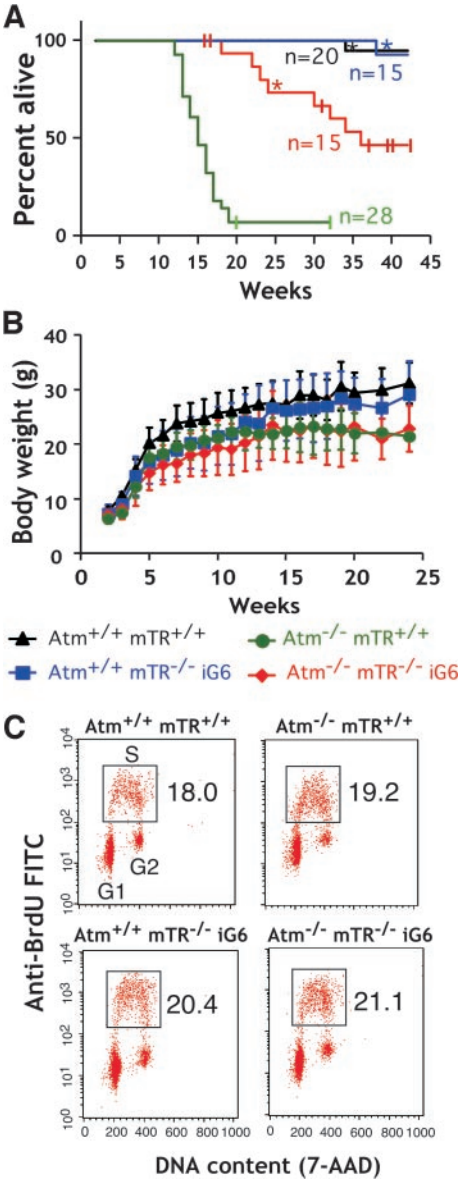

Fig. 4. Decreased and delayed incidence of thymic lymphoma in $Atm^{-/-}$ $mTR^{-/-}$ iG6 mice. *A*, Kaplan-Meier survival curve of $Atm^{+/+}$ $mTR^{+/+}$, $Atm^{+/+}$ $mTR^{-/-}$ iG6, $Atm^{-/-}$ $mTR^{-/-}$ iG6, and $Atm^{-/-}$ $mTR^{+/+}$ mice is shown. *Tick marks* indicate the current age of individual surviving mice. *, the mouse died without thymic lymphoma. *n* indicates the number of mice. *B*, similar growth rates were observed between $Atm^{-/-}$ $mTR^{-/-}$ iG6 and $Atm^{-/-}$ $mTR^{+/+}$ mice. The body weight of each cohort was followed over a period of 24 weeks. Each data point represents at least 7 individual mice, except for $Atm^{-/-}$ $mTR^{+/+}$ mice from week 20 only represents 1–2 surviving mice. *A* and *B* share the same legend. *C*, BrdUrd analysis of the bone marrow cells from young tumor-free mice shows no difference in cellular proliferation among four different genotypes. The *boxed area* refers to the BrdUrd+ cells that have been through or are still in S-phase. The numbers indicate the percentage of BrdUrd+ cells in the population. The data represent two independent experiments.

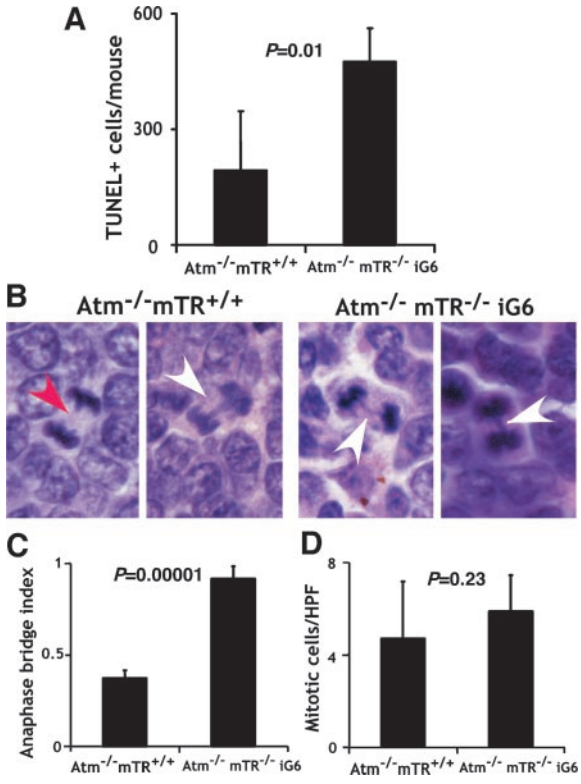

Fig. 5. Increased anaphase bridge index and apoptosis in the thymic lymphoma of $Atm^{-/-}$ $mTR^{-/-}$ iG6 mice. *A*, TUNEL+ cells were counted in four low power fields of each cohort (6 mice for $Atm^{-/-}$ $mTR^{+/+}$ and 4 mice for $Atm^{-/-}$ $mTR^{-/-}$ iG6). The average number of total TUNEL+ cells for each sample is shown. *B* and *C*, anaphases with anaphase bridges were counted in ten high power fields of each mouse (4 mice/cohort). Two representative images for each cohort are shown in *B*. *White arrowhead*, the anaphase with spanning bridges; *red arrowhead*, the normal anaphase. The anaphase bridge index represents the ratio of anaphases with at least 1 bridge to total number of anaphases counted in each mouse. A total of 77 and 50 anaphases were counted in $Atm^{-/-}$ $mTR^{+/+}$ and $Atm^{-/-}$ $mTR^{-/-}$ iG6 mice, respectively. *D*, cells undergoing mitosis with condensed chromatin were counted in 10 high-power fields of each mouse (4 mice/cohort). *Bars* represent the SD of the means from each mouse of each cohort.

were similar between $Atm^{-/-}$ $mTR^{+/+}$ and $Atm^{-/-}$ $mTR^{-/-}$ iG6 mice (Fig. 6*C*). Similarly, in the spleen, the percentages of mature $CD4^+$ and $CD8^+$ single-positive T cells were not significantly different between $Atm^{-/-}$ $mTR^{+/+}$ and $Atm^{-/-}$ $mTR^{-/-}$ iG6 mice (data not shown). Therefore, there is not a developmental block in the $Atm^{-/-}$ $mTR^{-/-}$ iG6 T cells at the transition from $CD4^-CD8^+$ immature, single-positive to $CD4^+CD8^+$ double-positive cells. Thus, we conclude that the tumors in the $Atm^{-/-}$ $mTR^{-/-}$ iG6 mice likely arise from an earlier developmental stage of the T-cell lineage than in the $Atm^{-/-}$ $mTR^{+/+}$ mice.

DISCUSSION

Telomere dysfunction is thought to mimic a DNA double-strand break and activate cell cycle arrest or apoptosis (53, 54). In cultured human cells, the cellular response to telomere dysfunction is both p53 and ATM dependent (8). Our study and the recent one by Wong *et al.* (31) indicate that Atm deficiency and short telomeres lead to increased apoptosis in mice, indicating that Atm is not required for cell death induced by progressive telomere shortening. The discrepancy in the requirement of Atm for apoptosis triggered by dysfunctional telomeres could be attributable to the differences in human *versus* mouse cells (55), the use of cultured cell lines *versus in vivo* models, or a mechanistic difference in how loss of telomere function through progressive telomere shortening *versus* loss of telomere binding proteins are recognized by the cell. If Atm is not required for apoptosis in response to telomere dysfunction, then other damage sensors such as Atr (56, 57) are likely to be involved. Recent data show that Atm and Atr act in distinct but partially overlapping pathways in response to specific types of DNA damage. Atm is more specialized for response to ionizing radiation, whereas Atr responds to a broad range of damage including ionizing radiation, UV, and stalled replication forks (58). In addition, unlike Atm, Atr binds to asynapsed chromosomes during meiosis (59, 60), suggesting that Atm and Atr may play a different role in recognition of DNA damage. Recent work in yeast suggests that Mec1 (Atr homolog), but not Tel1 (Atm homolog), is required for the cell cycle arrest of telomerase-deficient cells (61, 62).

The cooperative effect of Atm deficiency and short telomeres could be attributable to several causes. Telomere dysfunction sensitizes cells to ionizing radiation (63, 64), suggesting that the total amount of damage determines the cellular response. Thus, the increased apoptosis may result from the sensitizing effect of chromosome breaks that are present in the absence of Atm on the response to short telomeres. Alternatively, Atm loss may directly impair the residual protective function of short telomeres leading to increased telomere dysfunction. Our data support the latter model. In the $Atm^{-/-}$ $mTR^{-/-}$ iG6 and not the $Atm^{+/+}$ $mTR^{-/-}$ iG6 lymphocytes, there was an increase in end-to-end fusions consistent with increased telomere dysfunction but not with an additive effect of DNA breaks. We saw no increase in chromosome breaks in lymphocytes from $Atm^{-/-}$ $mTR^{-/-}$ iG6 mice compared with $Atm^{-/-}$ $mTR^{+/+}$ mice (Table 1). Furthermore, Atm clearly plays a direct role in telomere function in yeast. Absence of the Atm homolog Tel1 causes telomere shortening (20, 21), and loss of both the Atm and Atr homologs inhibits the ability of telomerase to elongate telomeres (23, 24). Recent work in yeast indicates a direct role for Tel1 in telomere protection (65). Thus, Atm may function at telomeres through direct binding to short telomeres, phosphorylation of telomere-binding proteins, or through a less direct regulation of the function of other telomere proteins. We propose that in the absence of Atm, the loss of this protection drives short telomeres to become prematurely dysfunctional without further shortening. The protection provided by Atm is not essential for long telomeres, perhaps because of the ample presence of telomere-binding proteins, such as TRF1, TRF2, or Pot1.

Several lines of evidence suggest that telomere dysfunction can limit tumor growth: (*a*) inhibition of telomerase in human cancer cells in culture leads to cell death (66–70); (*b*) double mutants of telomerase and $Ink4a/Arf^{-/-}$ resulted in a reduction of tumors in the late-generation mice with short telomeres (6); (*c*) telomere dysfunction enhances the chemotherapeutic effect on cancer cells (71); and (*d*) double-mutant APC^{min} $mTR^{-/-}$ late-generation mice show increased tumor initiation (microscopic adenomas) but decreased progression of the tumors into macroscopic adenomas (4). In support of the role of short telomeres in blocking tumor progression, this study and the work by Wong *et al.* (31) found a decrease in thymic lymphoma incidence in the Atm mTR double null mice. In addition, our double-mutant mice had a significant survival advantage. This difference in overall survival is likely attributable to the differing genetic background and/or mutagenesis strategies used in generating the Atm single-mutant mice (26, 29).

The observed reduction in thymic lymphoma incidence could be attributable to several different mechanisms: increased apoptosis, decreased tumor cell growth, delayed tumor initiation, or a combination of these factors. Our data suggest that the increased apoptosis attributable to the cooperative effect of short telomeres and Atm loss plays a major role in tumor reduction. Similar to the increased apoptosis seen in the germ cells in $Atm^{-/-}$ $mTR^{-/-}$ iG6 mice, we found increased apoptosis in the $Atm^{-/-}$ $mTR^{-/-}$ iG6 lymphomas compared with $Atm^{-/-}$ $mTR^{+/+}$ lymphomas. The significant increase

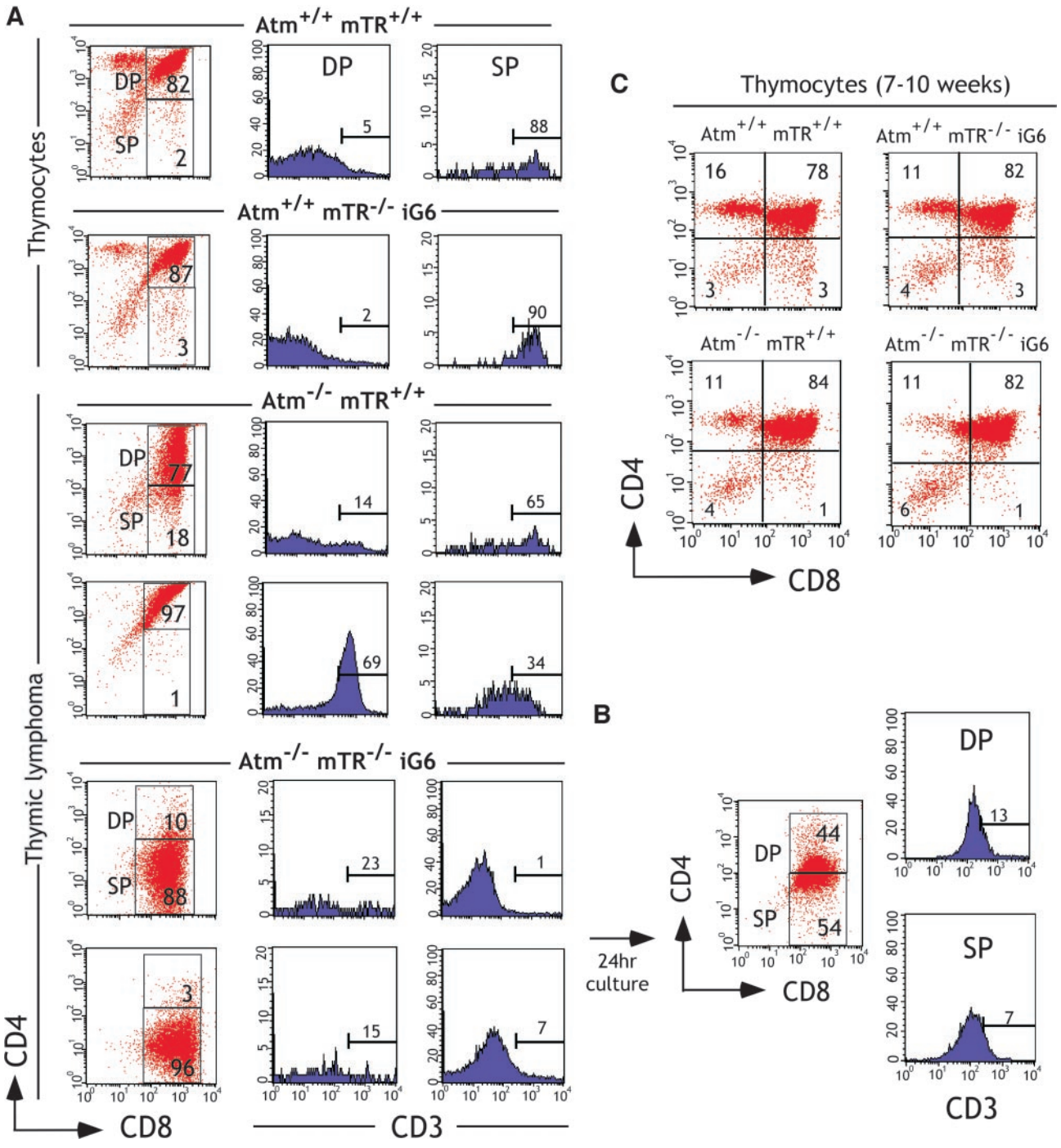

Fig. 6. Thymic lymphomas from $Atm^{-/-}$ $mTR^{-/-}$ iG6 mice are derived from $CD8^+$ immature, single-positive T cells. *A* and *B*, flow cytometric analysis on thymocytes and thymic lymphoma cells. *A*, fresh thymocytes from one control $Atm^{+/+}$ $mTR^{+/+}$ mouse and $Atm^{+/+}$ $mTR^{-/-}$ iG6 mouse and thymic lymphomas derived from two $Atm^{-/-}$ $mTR^{+/+}$ and $Atm^{-/-}$ $mTR^{-/-}$ iG6 mice were stained for CD4, CD8, and CD3. The $CD4^+CD8^+$ double-positive (*DP*) and $CD8^+$ single-positive (*SP*) cells were gated for expression of CD3. The percentages of DP, SP, and $CD3^+$ cells are indicated in each panel. *B*, thymic lymphomas from $Atm^{-/-}$ $mTR^{-/-}$ iG6 mice cultured for 24 h *in vitro* and stained for CD4, CD8, and CD3. The $CD4^+CD8^+$ double-positive (*DP*) and $CD8^+$ single-positive (*SP*) cells were gated for expression of CD3. *C*, T-cell development in the $Atm^{-/-}$ $mTR^{-/-}$ iG6 mice was similar to wild type. Thymocytes from tumor-free mice, 7–10 weeks of age, of four different genotypes were examined for CD4 and CD8 expression. The genotype is indicated on *top* of each panel. The percentage of each population is shown in each quadrant.

in anaphase bridges in the $Atm^{-/-}$ $mTR^{-/-}$ iG6 lymphomas indicates ongoing telomere dysfunction in the tumors. In contrast, the mitotic index in $Atm^{-/-}$ $mTR^{-/-}$ iG6 lymphomas was similar to $Atm^{-/-}$ $mTR^{+/+}$ mice, suggesting that decreased proliferation did not play a major role.

A decrease in tumor initiation might also contribute to the decreased latency of death from thymic lymphoma in $Atm^{-/-}$ $mTR^{-/-}$ iG6 mice. The switch in cell type from the $CD4^+CD8^+$ double-positive cells in $Atm^{-/-}$ to $CD8^+$ immature, single-positive cells in $Atm^{-/-}$ $mTR^{-/-}$ iG6 lymphomas suggests that tumors arise in a different cell population in $Atm^{-/-}$ $mTR^{-/-}$ iG6 mice. T-cell development progresses from a $CD4^-CD8^-$ double-negative stage through a $CD8^+$ immature, single-positive stage to $CD4^+CD8^+$ double-positive and further to mature $CD4^+$ or $CD8^+$ single-positive cells (46). The $CD8^+$ immature, single-positive cells represent 1–2% of developing T cells in thymus and are actively cycling (47–49, 72).

The developmental transition from immature, single-positive cells to double-positive cells involves a large clonal expansion (46). If the cycling and the expansion of immature, single-positive cells in $Atm^{-/-}$ $mTR^{-/-}$ iG6 mice are limited by telomere dysfunction, tumor initiation at the double-positive stage may be inhibited. Eventually however, sufficient instability may accumulate in the CD8 immature, single-positive cells and lead to tumor initiation. The delay in initiation may contribute to the increased latency of death attributable to thymic lymphoma in $Atm^{-/-}$ $mTR^{-/-}$ iG6 mice. Further analysis of the TCR rearrangements in these tumors will help pinpoint the specific subpopulation of cells that are transformed.

The increased survival of the $Atm^{-/-}$ $mTR^{-/-}$ iG6 mice provides a powerful model for the further study of A-T disease. In A-T patients, tumors account for only 10–15% of deaths, whereas the majority die from infections attributable to immunodeficiency (73). Although thymic lymphoma is the only tumor type seen in the $Atm^{-/-}$ mouse, A-T patients develop a variety of tumors including B-cell tumors and non-lymphoid tumors, such as ovarian, uterine, and stomach tumors (73, 74). The short life spans of the $Atm^{-/-}$ mice likely contribute to the phenotype difference with human A-T patients. The significant increase in the life span of the $Atm^{-/-}$ $mTR^{-/-}$ iG6 mouse will allow examination of the older $Atm^{-/-}$ $mTR^{-/-}$ iG6 mice and may thus provide insights into other clinical features of A-T patients.

ACKNOWLEDGMENTS

We thank Greider lab members, S. Desiderio, S. Ostrand-Rosenberg, M. Hemann, R. Yarrington, and R. Reed for discussions and comments on the manuscript; B. Todd and K. Kahn for technical assistance; and A. Wynshaw-Boris for the Atm PCR protocol.

REFERENCES

1. Blasco, M. A., Lee, H. W., Hande, M. P., Samper, E., Lansdorp, P. M., DePinho, R. A., and Greider, C. W. Telomere shortening and tumor formation by mouse cells lacking telomerase RNA. Cell, *91:* 25–34, 1997.
2. Rudolph, K. L., Chang, S., Lee, H. W., Blasco, M., Gottlieb, G. J., Greider, C., and DePinho, R. A. Longevity, stress response, and cancer in aging telomerase-deficient mice. Cell, *96:* 701–712, 1999.
3. Chin, L., Artandi, S. E., Shen, Q., Tam, A., Lee, S. L., Gottlieb, G. J., Greider, C. W., and DePinho, R. A. p53 deficiency rescues the adverse effects of telomere loss and cooperates with telomere dysfunction to accelerate carcinogenesis. Cell, *97:* 527–538, 1999.
4. Rudolph, K. L., Millard, M., Bosenberg, M. W., and DePinho, R. A. Telomere dysfunction and evolution of intestinal carcinoma in mice and humans. Nat. Genet., *28:* 155–159, 2001.
5. Artandi, S. E., Chang, S., Lee, S. L., Alson, S., Gottlieb, G. J., Chin, L., and DePinho, R. A. Telomere dysfunction promotes non-reciprocal translocations and epithelial cancers in mice. Nature (Lond.), *406:* 641–645, 2000.
6. Greenberg, R. A., Chin, L., Femino, A., Lee, K. H., Gottlieb, G. J., Singer, R. H., Greider, C. W., and DePinho, R. A. Short dysfunctional telomeres impair tumorigenesis in the INK4a(delta2/3) cancer-prone mouse. Cell, *97:* 515–525, 1999.
7. Gonzalez-Suarez, E., Samper, E., Flores, J. M., and Blasco, M. A. Telomerase-deficient mice with short telomeres are resistant to skin tumorigenesis. Nat. Genet., *26:* 114–117, 2000.
8. Karlseder, J., Broccoli, D., Dai, Y., Hardy, S., and de Lange, T. p53- and ATM-dependent apoptosis induced by telomeres lacking TRF2. Science (Wash. DC), *283:* 1321–1325, 1999.
9. Karlseder, J., Smogorzewska, A., and de Lange, T. Senescence induced by altered telomere state, not telomere loss. Science (Wash. DC), *295:* 2446–2449, 2002.
10. Lee, H. W., Blasco, M. A., Gottlieb, G. J., Horner, J. W., II, Greider, C. W., and DePinho, R. A. Essential role of mouse telomerase in highly proliferative organs. Nature (Lond.), *392:* 569–574, 1998.
11. Hemann, M. T., Rudolph, K. L., Strong, M. A., DePinho, R. A., Chin, L., and Greider, C. W. Telomere dysfunction triggers developmentally regulated germ cell apoptosis. Mol. Biol. Cell, *12:* 2023–2030, 2001.
12. Savitsky, K., Bar-Shira, A., Gilad, S., Rotman, G., Ziv, Y., Vanagaite, L., Tagle, D. A., Smith, S., Uziel, T., Sfez, S., *et al.* A single ataxia telangiectasia gene with a product similar to PI-3 kinase. Science (Wash. DC), *268:* 1749–1753, 1995.
13. Gatti, R. A., Berkel, I., Boder, E., Braedt, G., Charmley, P., Concannon, P., Ersoy, F., Foroud, T., Jaspers, N. G., Lange, K., *et al.* Localization of an ataxia-telangiectasia gene to chromosome 11q22–23. Nature (Lond.), *336:* 577–580, 1988.
14. Shiloh, Y., and Kastan, M. B. ATM: genome stability, neuronal development, and cancer cross paths. Adv. Cancer Res., *83:* 209–254, 2001.
15. Shiloh, Y. ATM and ATR: networking cellular responses to DNA damage. Curr. Opin. Genet. Dev., *11:* 71–77, 2001.
16. Rouse, J., and Jackson, S. P. Interfaces between the detection, signaling, and repair of DNA damage. Science (Wash. DC), *297:* 547–551, 2002.
17. Canman, C. E., Lim, D. S., Cimprich, K. A., Taya, Y., Tamai, K., Sakaguchi, K., Appella, E., Kastan, M. B., and Siliciano, J. D. Activation of the ATM kinase by ionizing radiation and phosphorylation of p53. Science (Wash. DC), *281:* 1677–1679, 1998.
18. Banin, S., Moyal, L., Shieh, S., Taya, Y., Anderson, C. W., Chessa, L., Smorodinsky, N. I., Prives, C., Reiss, Y., Shiloh, Y., and Ziv, Y. Enhanced phosphorylation of p53 by ATM in response to DNA damage. Science (Wash. DC), *281:* 1674–1677, 1998.
19. Tibbetts, R. S., Brumbaugh, K. M., Williams, J. M., Sarkaria, J. N., Cliby, W. A., Shieh, S. Y., Taya, Y., Prives, C., and Abraham, R. T. A role for ATR in the DNA damage-induced phosphorylation of p53. Genes Dev., *13:* 152–157, 1999.
20. Greenwell, P. W., Kronmal, S. L., Porter, S. E., Gassenhuber, J., Obermaier, B., and Petes, T. D. *TEL1*, a gene involved in controlling telomere length in *S. cerevisiae*, is homologous to the human ataxia telangiectasia gene. Cell, *82:* 823–829, 1995.
21. Morrow, D. M., Tagle, D. A., Shiloh, Y., Collins, F. S., and Hieter, P. *TEL1*, an *S. cerevisiae* homolog of the human gene mutated in ataxia telangiectasia, is functionally related to the yeast checkpoint gene *MEC1*. Cell, *82:* 831–840, 1995.
22. Naito, T., Matsuura, A., and Ishikawa, F. Circular chromosome formation in a fission yeast mutant defective in two ATM homologues. Nat. Genet., *20:* 203–206, 1998.
23. Chan, S. W., Chang, J., Prescott, J., and Blackburn, E. H. Altering telomere structure allows telomerase to act in yeast lacking ATM kinases. Curr. Biol., *11:* 1240–1250, 2001.
24. Craven, R. J., Greenwell, P. W., Dominska, M., and Petes, T. D. Regulation of genome stability by *TEL1* and *MEC1*, yeast homologs of the mammalian *ATM* and *ATR* genes. Genetics, *161:* 493–507, 2002.
25. Metcalfe, J. A., Parkhill, J., Campbell, L., Stacey, M., Biggs, P., Byrd, P. J., and Taylor, A. M. Accelerated telomere shortening in ataxia telangiectasia. Nat. Genet., *13:* 350–353, 1996.
26. Barlow, C., Hirotsune, S., Paylor, R., Liyanage, M., Eckhaus, M., Collins, F., Shiloh, Y., Crawley, J. N., Ried, T., Tagle, D., and Wynshaw-Boris, A. Atm-deficient mice: a paradigm of ataxia telangiectasia. Cell, *86:* 159–171, 1996.
27. Xu, Y., Ashley, T., Brainerd, E. E., Bronson, R. T., Meyn, M. S., and Baltimore, D. Targeted disruption of ATM leads to growth retardation, chromosomal fragmentation during meiosis, immune defects, and thymic lymphoma. Genes Dev., *10:* 2411–2422, 1996.
28. Elson, A., Wang, Y., Daugherty, C. J., Morton, C. C., Zhou, F., Campos-Torres, J., and Leder, P. Pleiotropic defects in ataxia-telangiectasia protein-deficient mice. Proc. Natl. Acad. Sci. USA, *93:* 13084–13089, 1996.
29. Borghesani, P. R., Alt, F. W., Bottaro, A., Davidson, L., Aksoy, S., Rathbun, G. A., Roberts, T. M., Swat, W., Segal, R. A., and Gu, Y. Abnormal development of Purkinje cells and lymphocytes in Atm mutant mice. Proc. Natl. Acad. Sci. USA, *97:* 3336–3341, 2000.
30. Spring, K., Cross, S., Li, C., Watters, D., Ben-Senior, L., Waring, P., Ahangari, F., Lu, S. L., Chen, P., Misko, I., Paterson, C., Kay, G., Smorodinsky, N. I., Shiloh, Y., and Lavin, M. F. Atm knock-in mice harboring an in-frame deletion corresponding to the human ATM 7636del9 common mutation exhibit a variant phenotype. Cancer Res., *61:* 4561–4568, 2001.
31. Wong, K. K., Maser, R. S., Bachoo, R. M., Menon, J., Carrasco, D. R., Gu, Y., Alt, F. W., and DePinho, R. A. Telomere dysfunction and Atm deficiency compromises organ homeostasis and accelerates ageing. Nature (Lond.), *421:* 643–648, 2003.
32. Hathcock, K. S., Hemann, M. T., Opperman, K. K., Strong, M. A., Greider, C. W., and Hodes, R. J. Haploinsufficiency of mTR results in defects in telomere elongation. Proc. Natl. Acad. Sci. USA, *99:* 3591–3596, 2002.
33. Hemann, M. T., Strong, M. A., Hao, L. Y., and Greider, C. W. The shortest telomere, not average telomere length, is critical for cell viability and chromosome stability. Cell, *107:* 67–77, 2001.
34. Lansdorp, P. M., Verwoerd, N. P., van de Rijke, F. M., Dragowska, V., Little, M. T., Dirks, R. W., Raap, A. K., and Tanke, H. J. Heterogeneity in telomere length of human chromosomes. Hum. Mol. Genet., *5:* 685–691, 1996.
35. Liyanage, M., Coleman, A., du Manoir, S., Veldman, T., McCormack, S., Dickson, R. B., Barlow, C., Wynshaw-Boris, A., Janz, S., Wienberg, J., Ferguson-Smith, M. A., Schrock, E., and Ried, T. Multicolour spectral karyotyping of mouse chromosomes. Nat. Genet., *14:* 312–315, 1996.
36. Barlow, C., Liyanage, M., Moens, P. B., Deng, C. X., Ried, T., and Wynshaw-Boris, A. Partial rescue of the prophase I defects of Atm-deficient mice by p53 and p21 null alleles. Nat. Genet., *17:* 462–466, 1997.
37. Burkitt, H. G., Young, B., and Heath, J. W. Wheater's Functional Histology: A Text and Color Atlas, Ed. 3, pp. 323–327. New York: Churchill Livingstone, 1993.
38. Enders, G. C., and May, J. J. Developmentally regulated expression of a mouse germ cell nuclear antigen examined from embryonic day 11 to adult in male and female mice. Dev. Biol., *163:* 331–340, 1994.
39. Chapman, D. L., and Wolgemuth, D. J. Expression of proliferating cell nuclear antigen in the mouse germ line and surrounding somatic cells suggests both proliferation-dependent and -independent modes of function. Int. J. Dev. Biol., *38:* 491–497, 1994.
40. Liyanage, M., Weaver, Z., Barlow, C., Coleman, A., Pankratz, D. G., Anderson, S., Wynshaw-Boris, A., and Ried, T. Abnormal rearrangement within the alpha/delta T-cell receptor locus in lymphomas from Atm-deficient mice. Blood, *96:* 1940–1946, 2000.
41. Westphal, C. H., Rowan, S., Schmaltz, C., Elson, A., Fisher, D. E., and Leder, P. Atm and p53 cooperate in apoptosis and suppression of tumorigenesis, but not in resistance to acute radiation toxicity. Nat. Genet., *16:* 397–401, 1997.

42. McClintock, B. The stability of broken ends of chromosomes in *Zea mays*. Genetics, *26:* 234–282, 1941.
43. Kirk, K. E., Harmon, B. P., Reichardt, I. K., Sedat, J. W., and Blackburn, E. H. Block in anaphase chromosome separation caused by a telomerase template mutation. Science (Wash. DC), *275:* 1478–1481, 1997.
44. Xu, Y., Yang, E. M., Brugarolas, J., Jacks, T., and Baltimore, D. Involvement of p53 and p21 in cellular defects and tumorigenesis in *Atm*−/− mice. Mol. Cell. Biol., *18:* 4385–4390, 1998.
45. Kang, J., Bronson, R. T., and Xu, Y. Targeted disruption of NBS1 reveals its roles in mouse development and DNA repair. EMBO J., *21:* 1447–1455, 2002.
46. Janeway, C. A., Jr., Travers, P., Walport, M., and Shlomchik, M. Immunobiology: The Immune System in Health & Disease, Ed. 5, pp. 7:1–35. New York: Garland Publishing Inc., 2001.
47. Paterson, D. J., and Williams, A. F. An intermediate cell in thymocyte differentiation that expresses CD8 but not CD4 antigen. J. Exp. Med., *166:* 1603–1608, 1987.
48. MacDonald, H. R., Budd, R. C., and Howe, R. C. A CD3- subset of CD4−8+ thymocytes: a rapidly cycling intermediate in the generation of CD4+8+ cells. Eur. J. Immunol., *18:* 519–523, 1988.
49. Shortman, K., Wilson, A., Egerton, M., Pearse, M., and Scollay, R. Immature CD4− CD8+ murine thymocytes. Cell. Immunol., *113:* 462–479, 1988.
50. Guidos, C. J., Weissman, I. L., and Adkins, B. Intrathymic maturation of murine T lymphocytes from CD8+ precursors. Proc. Natl. Acad. Sci. USA, *86:* 7542–7546, 1989.
51. Wilson, A., Petrie, H. T., Scollay, R., and Shortman, K. The acquisition of CD4 and CD8 during the differentiation of early thymocytes in short-term culture. Int. Immunol., *1:* 605–612, 1989.
52. Petrie, H. T., Hugo, P., Scollay, R., and Shortman, K. Lineage relationships and developmental kinetics of immature thymocytes: CD3, CD4, and CD8 acquisition *in vivo* and *in vitro*. J. Exp. Med., *172:* 1583–1588, 1990.
53. de Lange, T. Telomere dynamics and genome instability in human cancer. *In:* E. H. Blackburn and C. W. Greider (eds.), Telomere, Vol. 10, pp. 263–293. Woodbury, NY: Cold Spring Harbor Laboratory Press, 1995.
54. Blackburn, E. H. Switching and signaling at the telomere. Cell, *106:* 661–673, 2001.
55. Smogorzewska, A., and de Lange, T. Different telomere damage signaling pathways in human and mouse cells. EMBO J., *21:* 4338–4348, 2002.
56. Bentley, N. J., Holtzman, D. A., Flaggs, G., Keegan, K. S., DeMaggio, A., Ford, J. C., Hoekstra, M., and Carr, A. M. The *Schizosaccharomyces pombe rad3* checkpoint gene. EMBO J., *15:* 6641–6651, 1996.
57. Cimprich, K. A., Shin, T. B., Keith, C. T., and Schreiber, S. L. cDNA cloning and gene mapping of a candidate human cell cycle checkpoint protein. Proc. Natl. Acad. Sci. USA, *93:* 2850–2855, 1996.
58. Zhou, B. B., and Elledge, S. J. The DNA damage response: putting checkpoints in perspective. Nature (Lond.), *408:* 433–439, 2000.
59. Keegan, K. S., Holtzman, D. A., Plug, A. W., Christenson, E. R., Brainerd, E. E., Flaggs, G., Bentley, N. J., Taylor, E. M., Meyn, M. S., Moss, S. B., Carr, A. M., Ashley, T., and Hoekstra, M. F. The Atr and Atm protein kinases associate with different sites along meiotically pairing chromosomes. Genes Dev., *10:* 2423–2437, 1996.
60. Barlow, C., Liyanage, M., Moens, P. B., Tarsounas, M., Nagashima, K., Brown, K., Rottinghaus, S., Jackson, S. P., Tagle, D., Ried, T., and Wynshaw-Boris, A. Atm deficiency results in severe meiotic disruption as early as leptonema of prophase I. Development (Camb.), *125:* 4007–4017, 1998.
61. Enomoto, S., Glowczewski, L., and Berman, J. MEC3, MEC1, and DDC2 are essential components of a telomere checkpoint pathway required for cell cycle arrest during senescence in *Saccharomyces cerevisiae*. Mol. Biol. Cell, *13:* 2626–2638, 2002.
62. IJpma, A. S., and Greider, C. W. Short telomeres induce a DNA damage response in *Saccharomyces cerevisiae*. Mol. Biol. Cell, *14:* 987–1001, 2003.
63. Wong, K. K., Chang, S., Weiler, S. R., Ganesan, S., Chaudhuri, J., Zhu, C., Artandi, S. E., Rudolph, K. L., Gottlieb, G. J., Chin, L., Alt, F. W., and DePinho, R. A. Telomere dysfunction impairs DNA repair and enhances sensitivity to ionizing radiation. Nat. Genet., *26:* 85–88, 2000.
64. Goytisolo, F. A., Samper, E., Martin-Caballero, J., Finnon, P., Herrera, E., Flores, J. M., Bouffler, S. D., and Blasco, M. A. Short telomeres result in organismal hypersensitivity to ionizing radiation in mammals. J. Exp. Med., *192:* 1625–1636, 2000.
65. Chan, S. W., and Blackburn, E. H. Telomerase and ATM/Tel1p protect telomeres from nonhomologous end joining. Mol. Cell, *11:* 1379–1387, 2003.
66. Hahn, W. C., Stewart, S. A., Brooks, M. W., York, S. G., Eaton, E., Kurachi, A., Beijersbergen, R. L., Knoll, J. H., Meyerson, M., and Weinberg, R. A. Inhibition of telomerase limits the growth of human cancer cells. Nat. Med., *5:* 1164–1170, 1999.
67. Zhang, X., Mar, V., Zhou, W., Harrington, L., and Robinson, M. O. Telomere shortening and apoptosis in telomerase-inhibited human tumor cells. Genes Dev., *13:* 2388–2399, 1999.
68. Damm, K., Hemmann, U., Garin-Chesa, P., Hauel, N., Kauffmann, I., Priepke, H., Niestroj, C., Daiber, C., Enenkel, B., Guilliard, B., Lauritsch, I., Muller, E., Pascolo, E., Sauter, G., Pantic, M., Martens, U. M., Wenz, C., Lingner, J., Kraut, N., Rettig, W. J., and Schnapp, A. A highly selective telomerase inhibitor limiting human cancer cell proliferation. EMBO J., *20:* 6958–6968, 2001.
69. White, L. K., Wright, W. E., and Shay, J. W. Telomerase inhibitors. Trends Biotechnol., *19:* 114–120, 2001.
70. Shammas, M. A., Simmons, C. G., Corey, D. R., and Shmookler Reis, R. J. Telomerase inhibition by peptide nucleic acids reverses "immortality" of transformed human cells. Oncogene, *18:* 6191–6200, 1999.
71. Lee, K. H., Rudolph, K. L., Ju, Y. J., Greenberg, R. A., Cannizzaro, L., Chin, L., Weiler, S. R., and DePinho, R. A. Telomere dysfunction alters the chemotherapeutic profile of transformed cells. Proc. Natl. Acad. Sci. USA, *98:* 3381–3386, 2001.
72. Verbeek, S., Izon, D., Hofhuis, F., Robanus-Maandag, E., te Riele, H., van de Wetering, M., Oosterwegel, M., Wilson, A., MacDonald, H. R., and Clevers, H. An HMG-box-containing T-cell factor required for thymocyte differentiation. Nature (Lond.), *374:* 70–74, 1995.
73. Taylor, A. M., Metcalfe, J. A., Thick, J., and Mak, Y. F. Leukemia and lymphoma in ataxia telangiectasia. Blood, *87:* 423–438, 1996.
74. Morrell, D., Cromartie, E., and Swift, M. Mortality and cancer incidence in 263 patients with ataxia-telangiectasia. J. Natl. Cancer Inst., *77:* 89–92, 1986.